Microstructural Analysis and Optimization of Asbestos Free Brake Pad

Vinayak Arun Sankar VIJAYASANKAR [1] *, Suresh PARAMASIVAM [2]

[1] *Department of Mechanical Engineering, Karpagam College of Engineering, Coimbatore -641032, India*
[2] *Department of Mechanical Engineering, Muthayammal Engineering College, Namakkal -637408, India*

http://doi.org/10.5755/j02.ms.37951

Received 9 July 2024; accepted 20 November 2024

A friction lining material that is free of asbestos has been developed using sea shell powder (with a diameter of 125 μm), phenolic resin as the binder, and alumina metal filings and graphite as fillers. Prior to pulverization, the sea shells were oven-cured at 100 °C for five hours to eliminate excess moisture. The resulting pulverized sea shell, along with phenolic resin, alumina metal filings, and graphite, was used to create samples, which were evaluated according to the ASTM D 4703-03 standard. The newly developed asbestos-free brake pads incorporating sea shell powder (SS) and four other components underwent physical, chemical, and Thermal Gravimetric-Differential Thermal Analysis (TG-DTA) assessments, comparing them with commercial brake pad materials. Morphological examinations of worn surfaces indicated various forms of wear, including abrasion, adhesion, grooving, and delamination. Scanning Electron Microscope (SEM) images showed that the worn surfaces of the composite with 35 wt.% SS powders exhibited a smoother finish with fewer cracks, suggesting reduced wear. Taguchi's analytical approach (L16 orthogonal array) was employed to assess the coefficient of friction and wear rate under different tribological parameters. Additionally, a statistical analysis of variance (ANOVA) was conducted to identify significant compositions for optimal brake lining performance. The ANOVA tables revealed that the regression models were valid as the P-values were less than 0.05 for a confidence level of 95 %.
Keywords: seashell (SS), brake linings, morphological studies, friction materials.

1. INTRODUCTION

The current research work is done to understand the wear mechanisms of the friction materials and improve their wear and frictional properties. When using a disc brake, the linings, which are often referred to as pads, grip the disc from opposing sides. The normal forces exerted by the pads are unaffected by the frictional force that acts between them and the disc as these forces are perpendicular to one another. Therefore, the amount of force required to apply the brakes will be proportional to the amount of normal force that is delivered, provided that the coefficient of friction between the two components remains unchanged. One other advantage is the reduced overall weight [1].

In automotive industry the trend has shifted to asbestos free organic composite friction materials manufacture brake disc pads and clutch facing are increasingly growing in demand used in automotive applications. They are essentially multi-ingredient systems to achieve the desired amalgam of performance properties [2] amongst which the coefficient of friction and its stability under various operating conditions, such as temperature, pressure and speed is most important. The four categories of ingredients, viz. binders, fibers, friction modifiers and fillers based on the major function they perform apart from contributing towards friction and wear performance are selected [3]. Binders mainly from phenolics or modified phenolics provide mechanical integrity to the friction material while fibers, such as mineral, ceramics, organic and metallic types provide mainly the strength. Friction modifiers, such as abrasives and solid lubricants are used to achieve the desired range of friction. Fillers are again subdivided as functional fillers and space fillers/inert fillers. The effect of such ingredients on tribo-performance and fade and recovery behaviour is extensively studied in the literature [4-10]. In the case of a brake lining, the control of the friction characteristics by changing the ingredients is a very complicated task, since it requires many experiments to obtain reliable results and involves synergistic effects from multiple ingredients. A limited number of studies investigating the compositional effect are available in the literature [11-15] and a complete analysis concerning all the ingredients in a friction material is seldom found. The limited information about ingredients used in the friction material and their effects on the friction characteristics is partly ascribed to proprietary reasons [16-18]. In this work, a friction material containing 16 different ingredients was investigated to study the effect of ingredients on the friction characteristics. We focused on the change of the average friction coefficient, fade, wear rate, and friction induced noise propensity as a function of the relative amount of the ingredient.

2. MATERIAL AND METHODS

2.1. Filler material

As their natural habitat is the ocean, seashells naturally possess a high resilience to moisture. They are naturally endowed with superior attributes of hardness and corrosion resistance, which in turn, endows them with an increased resistance to wear [19]. This is the primary reason why the powder made from seashells was chosen to be used as a

* Corresponding author: V.A.S. Vijayasankar
E-mail: *arunsankar@kce.ac.in*

filler material in the production of this composite. Additionally, since the seashell powders are ball-milled and turned into powders, they can fill the micropores of the composites that are formed while the composites are curing. It renders the composites defect-free, and when a material is defect-free, it has superior qualities in terms of both its mechanics and its physics. The seashell for this research was collected from the beaches of Tuticorin in the state of Tamil Nadu, India. Studies carried out by the researchers who fabricated and tested a glass fiber reinforced epoxy composite filled with seashell found out that the composite can be used for making auto parts, helmets, and other similar items [20]. However, they also found that the addition of the seashell fillers reduces the tensile properties of the composites.

2.2. Reinforcement

To strengthen the material, this research makes use of steel powder as reinforcement. Steel powder is often employed in commercial semi-metallic brake pads because they offer high wear resistance and retain friction at increased temperatures. This led to their selection as the material of choice [21]. Steel powder offers good traction, but it does not prevent fade and causes the disc plate and brake pads to wear down at about the same rate, which is problematic since the brake pad, not the disc plate, is intended to be a consumable component. Additionally, steel powder was acquired from Sarada Industries in Jaipur, India.

2.3. Lubricant

Graphite, which is a polymorphic form of carbon, has one-of-a-kind physical and chemical features that make it very useful in the high-tech industrial sector. It is possible to achieve above 99.99 % purity using thermal or chemical purification on a large industrial scale with outcomes that are both easy and inexpensive to achieve. It has a high melting temperature of 3,500 °C, is a great heat and electrical conductor, and has a high melting temperature [22]. It is chemically inert, exceedingly refractory, and resistant to the effects of high temperatures. Additionally, the graphite that was used in this investigation came from Sarada Industries in Jaipur, India.

2.4. Abrasive

Within the family of engineering ceramics, alumina is the material that is used the most often and has the lowest overall cost. As a consequence of this ceramic's widely accessible raw ingredients, which are of a high performance and technical grade, and their reasonable price, the process of producing alumina forms results in overall superior value [23]. It should not come as a surprise that fine grain technical grade alumina has a very broad variety of applications since it has a superb mix of characteristics and an appealing price. In addition, the alumina that was used in this investigation was acquired from Kumaraswamy Chemicals in Cuddalore, Tamilnadu, India.

Table 1 presents with the reasons behind choosing the specific filler, reinforcement, lubricant, binder and abrasive materials.

Table 1. Material used and reason for their choices [24]

No.	Role	Material	Reason
1.	Material	Sea Shell	Rarely used Non-asbestos eco-friendly material Improves resilience in the binder system and reduces brake noise
2.	Binder	Phenolic resin	Good wettability and low cost Temperature resistance up to 250ºC Having good thermal, mechanical, and tribology properties.
3.	Abrasive	Alumina	Low cost Better wear properties.
4.	Friction Modifier	Graphite	Non-hazardous, Cheap and widely used
5.	Reinforcement	Steel powder	High wear resistance

2.5. Formulation

Table 2 presents the formulation of the friction composites that were used for this research project. Table 2 displays the quantities (expressed as a percentage) of each constituent that are included in the composite material. Because the presence of relatively dominating filler may have a considerable influence on the final qualities of the brake pads, this mix of composite materials for the composite was selected because of it. This formulation was selected because it is most similar to the usual formulation indicated, which is also the formulation that is commonly utilized in the majority of the basic formulations of commercial brake pads [25].

Table 2. Percentage of materials used in the brake pad samples [25]

ID	Materials, wt.%				
	SS	Resin	Alumina	Graphite	Steel powder
SS20	20	63	7	5	5
SS25	25	58	7	5	5
SS30	30	53	7	5	5
SS35	35	48	7	5	5

2.6. Crushing

To reduce the size of the solid pieces that needed to be crushed, a jaw crusher was used to perform the crushing operation.

Fig. 1. Samples of crushed sea shells [24]

2.7. Sieving

An UTS Sieve shaker was used for the purpose of screening the crushed and ground sea shell. Sieving is a process or operation used to separate specified sizes of crushed and sea shell from a mix of varied sizes [26]. This is accomplished by passing the palm slag through a series of meshes of varying sizes. In this study, a stacking type sieve was used to produce a range of particle sizes. The sea shell is sent through a succession of sieves that are stacked in sequence, beginning with the sieve that has the smallest apertures and working its way up to the sieve that has the largest openings. The 125 μm wide seashell as shown in Fig. 1 was selected as the best option for the objectives of this study. When the diameter of the particles was smaller than the size of the square aperture on the sieve screen, they were able to pass through the sieve. The particles that were sieved were roughly spherical and irregular in form. According to Jain's research, sieve size does not reliably predict mass-based findings for elongated and flat particles since these particles can still pass through or may pass through the screen end-on, despite the fact that they are unable to pass through the screen side-on [27].

2.8. Sample preparation

Mixing, preforming, post curing, and surface finishing were the steps involved in the manufacturing process of brake friction compounds. The process began with several components and finished with surface finishing. Table 3 outlines the steps that must be taken to successfully manufacture brake friction material.

Table 3. Outline of the preparation steps

Steps	Process
Mixing	Sequential mixing of all ingredients in plough type shear mixture
Preforming and curing	Hot Compaction of the mixed ingredients
Post curing	Cured products further cured to remove the excess uncured resin content
Finishing	Grinding and center cut on finished brake pads

During this investigation, powder was compacted using the cold press method, with the required instruments and dies. Powder is often placed inside of a die chamber that is closed off at one end. After the various components of the brake pad had been milled into a homogenous mixture, this mixture was prepared to be put in the mold and compressed.

However, in order to prevent the powder from sticking to the surface of the mould, a lubricant such as WD-40 was sprayed on the mould before it was filled with the powder [28]. This served to both lubricate the mould and prevent the powder from adhering to the surface of the mould. After the lubricant had been applied to the mould, the homogenous mixture of materials that had been created by the ball mill was deposited in the mould and compressed using a uniaxial hydraulic compression machine with a pressure of 15 – 17 MPa. The compaction procedure resulted in the production of brake pad components that, after cooled to room temperature, could be compressed into the form of the mould, and the resulting compacted materials could then be expelled from the die cavity. Each of the specimens was compressed until it took on the appropriate form and had a diameter of 10 mm as shown in Fig. 2. The blueprint for the mould served as the basis for determining their final dimensions and contours. Green bodies are the samples that have been compressed, and they belong to the category of brake pad composite materials. These green bodies were compressed even deeper and then allowed to cure.

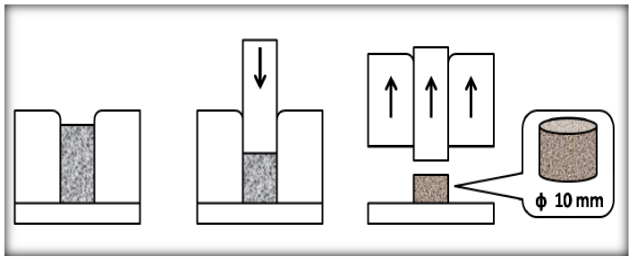

Fig. 2. Schematic image of showing technique for the preparation of the 'green body' samples [24]

The green body was allowed to cure until the pad binder system had reached its maximum curing potential and solidified into a block. The green body was heated by being subjected to certain pressures in a hot press. 60 tons of pressure was used throughout the moulding process. Table 4 indicates the post curing temperature that was set in the hot press. After the post curing process had run its course for 5 minutes, the samples were left out in the open air to cool to room temperature.

Table 4. Post curing temperatures [29]

Cycles	Temperature, °C
I	90 – 100
II	105 – 120
III	125 – 140
IV	145 – 160

Before and after the curing procedure, the diameters of the samples were measured using a vernier calliper, and they were weighed using a balance to ensure accuracy. Calculating the percentage of change in the dimensions of the samples required the measurements to be taken, which were then employed. In this instance, changes in the material's physical qualities were brought on by chemical interactions that took place between the raw ingredients as the phenolic resin was being heated to its curing temperature. Following the completion of the post curing process, the friction composites were taken out of the oven. Grinding wheels were used on the friction composites to attain the appropriate thickness and to remove the resinous skin from the surface of the friction composites. This was accomplished by grinding the friction composites. Fig. 3 depicts the brake pads that were ultimately created.

3. RESULTS AND DISCUSSION

3.1. Microstructure analysis

Scanning Electron Microscope (SEM) JEOL JSM 6390LV, a high-performance, low-cost instrument was used to create the microstructure image of the brake pad sample after it had been cured. The microscope had a high resolution of 3.0 nm and a magnification of 100 times. The SEM micrographs of

the brake pad sample are shown in Fig. 4, and each one displays a different proportion of phenolic resin and sea shell powder.

Fig. 3. Samples of finished brake pads [24]

The images depict the carbon black materials that were used as a lubricant for the brake pad composite matrix. The black dots in the images indicate the carbon black ingredients, and the carbon region shows an area that had a combination of phenolic resin and carbon black. On the other hand, the pale zone and the dots point to calcium carbonate being present [30].

Although there are some signs of holes owing to the varying particle size of each admixture material, overall inspection reveals that the combination of the components for the brake pad is well disseminated. This is the case even if there are some pores. The micrograph showed that the mixture with the ratio 20 – 25 included a greater number of holes than the combination with the ratios 30 and 35. It has been shown that the quantity of phenolic resin and powdered sea shells both have a role in determining the existence of pores. The pores shrunk as the amount of phenolic resin and sea shell powder in the mixture increased; this can be seen clearly in photographs that have been processed to reduce the number of holes [31].

Following the completion of the wear testing, the worn surfaces of the brake pad composites were analysed by SEM. On a microscopic scale, the worn surfaces gave the impression of being rough, and the texture was described as having peaks and valleys. During the braking test, wear debris was produced, and it consisted basically of a fine powder that was either discharged into the environment or confined between the contact regions or in void areas [32]. During the test, wear debris was formed. The debris from the wear collected, heaped up against the places that came into contact. Following this, the contact regions grew in size and produced a friction layer as a result of the compaction of the debris that had been trapped [33]. The worn surface of the sample can be seen in most of the SEM micrographs that are shown in Fig. 5. This micrograph portrays that the built-up friction layer was only present on sections of the surface. As can be seen in Fig. 5, the friction layer does not completely cover the SS particles and the filled resin. The debris has a tendency to fill the gaps and holes that were caused as a consequence of the poor compactness that was a direct result of the low moulding pressures [34].

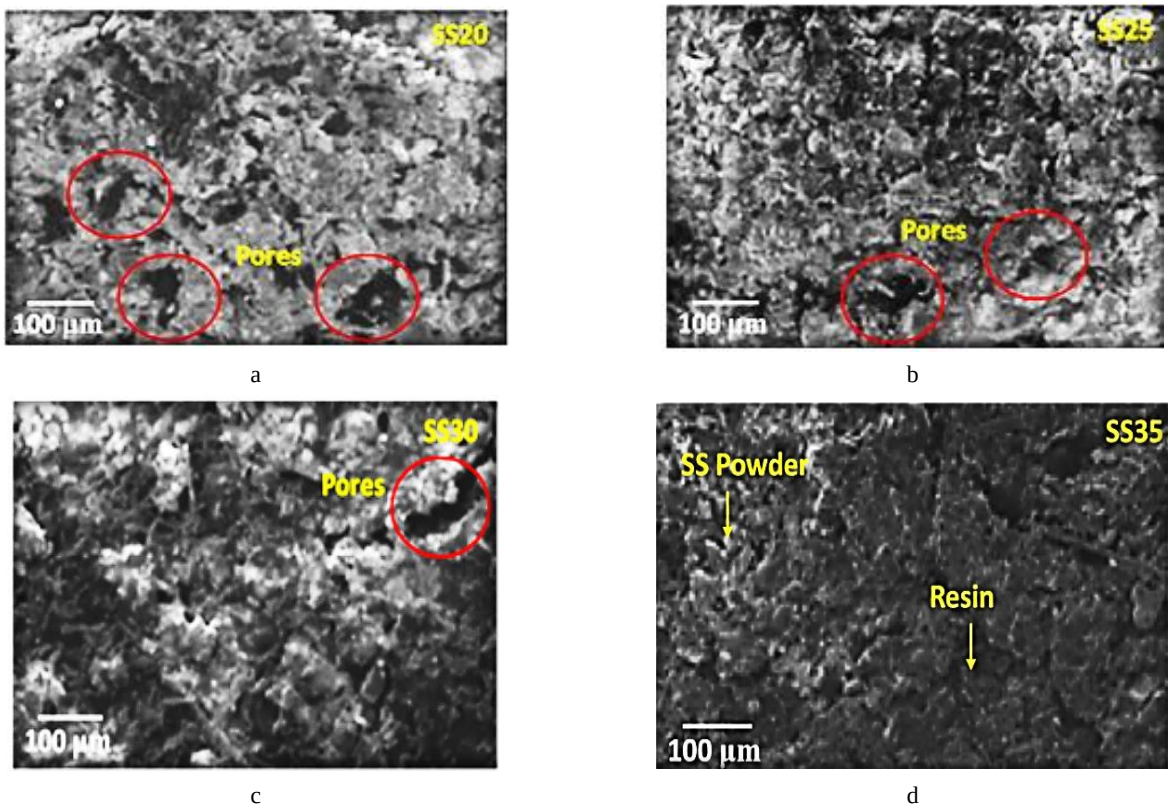

Fig. 4. a – presence of pores in SS 20 samples; b – presence of pores in SS 25 samples; c – presence of pores in SS 30 samples d – no presence of pores in SS 35 samples

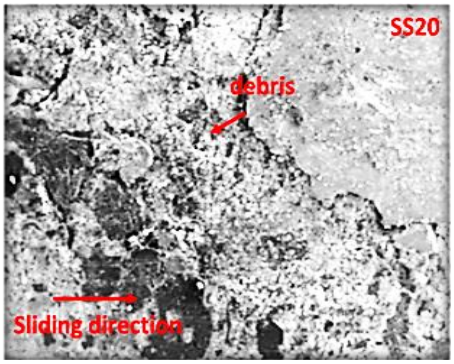

a

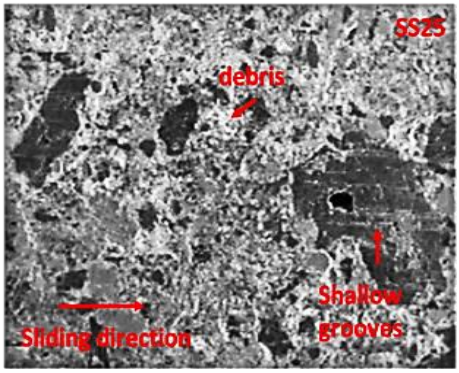

b

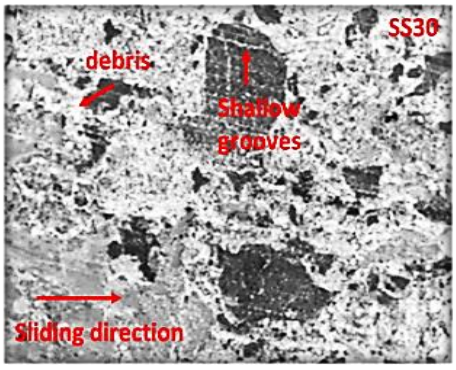

c

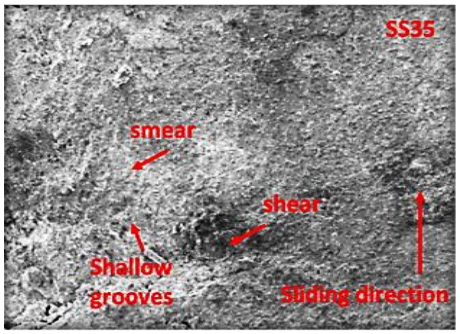

d

Fig. 5. Worn-wear test microstructure of SS brake pad samples prepared with sea shell: a – 20 %; b – 25 %; c – 30%; d – 35 %

From the SEM micrographs taken during the wear test, the following types of wear processes were detected and involved: abrasion, adhesion, and groove development. The abrasion wear mechanism is usually defined by the presence of ploughed marks on the friction layers. This is because abrasion wear occurs when two surfaces rub against one another. This wear mechanism was seen in all instances of the wear test for all the samples as shown in Fig. 5. This occurs because of hard particles ploughing into the wear surface, which exists as a third component between the friction material and the brake disc [35]. Another wear process that is involved is adhesion, which takes place when the contact area expands to create patches because of the compaction of wear debris that is trapped between the sliding surfaces. This happens when the contact area is subjected to friction. As demonstrated in Fig. 5, a thin film will continually create smear and shear on the sliding surface as the braking process continues. This will result in the film becoming flatter. This friction film has a composition that is comparable to those of the elements found in brake discs and friction material.

3.2. Surface roughness

The three-dimensional surface roughness profile of the worn-out friction pads may be seen in Fig. 6. When temperatures are raised to high levels, thermal stresses emerge at the mating contact. These stresses cause the fibers to become thinner. It causes friction undulations, which leads to an increase in the roughness of the friction surface. Because of the lubricating films made of SS that were present in the frictional surface, the composites SS20 and SS25 exhibited decreased surface roughness.

Brake pad surfaces undergo deformation during contact, and certain abrasions might lead to excessive wear owing to the pad's heterogeneous composition. The adhesion process destroys the pore walls and creates 1 – 2 μm high plateaus in the non-adherent zones.

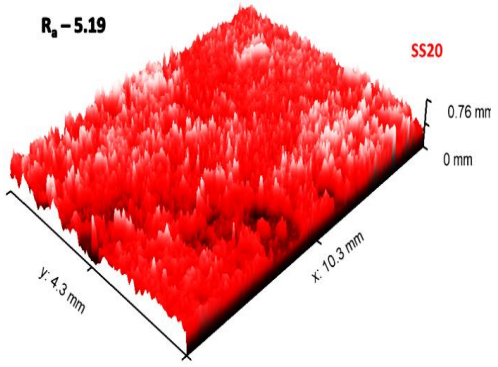

a

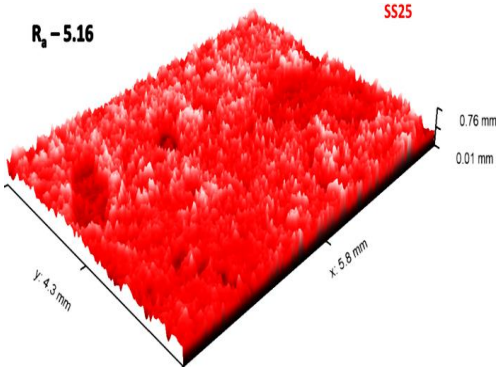

b

continued on the next page

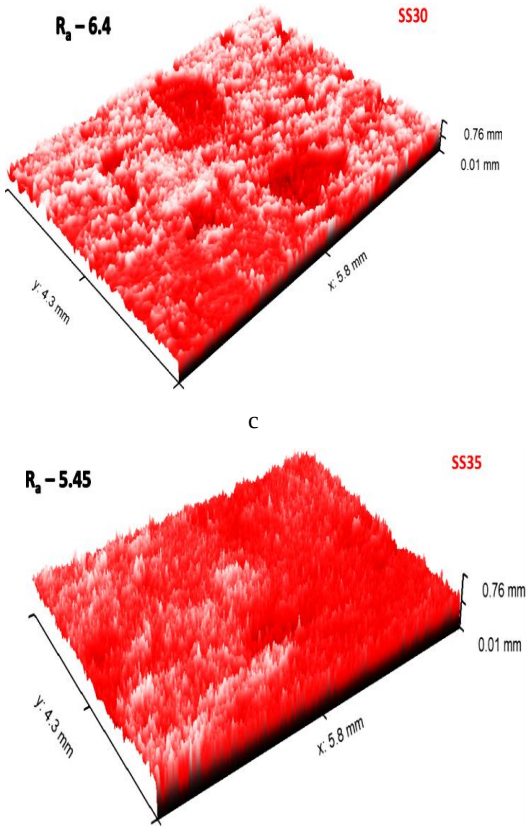

Fig. 6. Surface roughness of composite: a – SS20; b – SS25; c – SS30; d – SS35

Fig. 6 c depicts the major impact plot for the minimal wear rate. The longer line represents the most influential element, and the addition of the filler powder is shown next to it on the plot, which was constructed using the "smaller is better" aim [36]. From the graph, it was observed that the SS powders added should be as high as possible; this variable has the most impact. Phenolic resin, which decomposes at about 450 °C, is the ideal binder for brake pad production. Utilizing a 100 μm sieve of SS powder with 70 % and 30 % composition of resin, the findings indicated superior results for the fabrication of brake pads than those seen in the literature for an asbestos brake pad using agro waste and phenolic resin as binder [16].

The generated samples lost hardness, density, and compressive strength as the sieve grade became smaller, but the wear rate got larger as indicated in Fig. 7. The brake pad material's improved characteristics may be attributed to its increasingly tiny sieve particle size. The present research evaluates the rate of wear on brake pads as well as their composition in the context of the above factors.

3.3. Thermal gravimetric analysis (TGA)

Perkin Elmer made TGA4000 was used to test the substance's thermal stability [37]. It was used for determining whether the completed product had lost weight in proportion to an increase in temperature. A weight of roughly 5 mg was assigned to the sample. The rate of gas flow was 20 ml/min, and the gas that was being used was air. The rate of temperature increase was 10 °C/min, and the highest test temperature that was being used was 800 °C. The platinum pan that was being used was 180 μL. The results of TGA for brake pads containing different percentages of seashells are shown in Fig. 8.

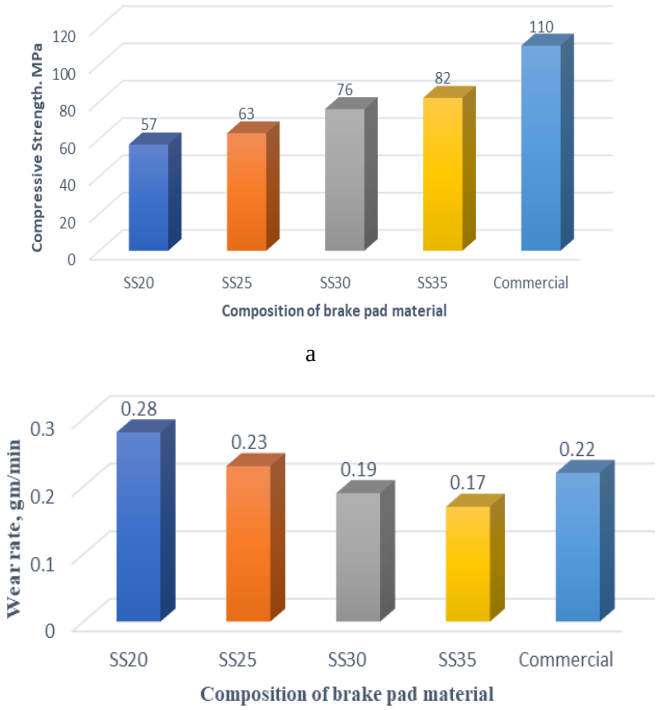

Fig. 7. a – compressive strength of the SS compositions compared with a commercial brake pad; b – wear rate of the SS compositions compared with a commercial brake pad

It is possible that the high thermal characteristics of commercial samples are due to the presence of asbestos fibers, which were often found in them. The degradation curve of the seashell brake pads was comparable, although it was variable depending on the temperature. Below 200 °C, deterioration starts in earnest. It seems, after thorough inspection, that the temperature at which heat deterioration occurred was between 140 °C and 170 °C. An apparent peak in the rate of degradation can be seen at around 641 °C for SS20, SS25, and SS30 in the seashell-filled brake pad. This peak moves to 460 °C for SS35 because of an increase in the amount of seashell content.

This leads one to believe that a higher temperature was necessary for the phenol contained in the seashell composites to go through the process of thermal decomposition. The addition of seashell to phenolic resin resulted in a significant increase in the resin's thermal stability, and this was not just because seashells themselves have a higher thermal stability. It has been discovered that seashells contain between 95 and 99 % calcium carbonate ($CaCO_3$) by weight, which is the reason why they are so successful [38]. At temperatures of 500 °C, alumina begins to degrade in tests of seashell-filled brake pads. Researchers have shown that alumina goes through a process of thermal degradation between temperatures of 400 °C and 500 °C, which reveals a potential way for the additive fabrication of dense and resilient ceramic structures. The graphite in iron-filled brake pads, on the other hand, underwent thermal decomposition within a temperature range of 700 °C and 800 °C.

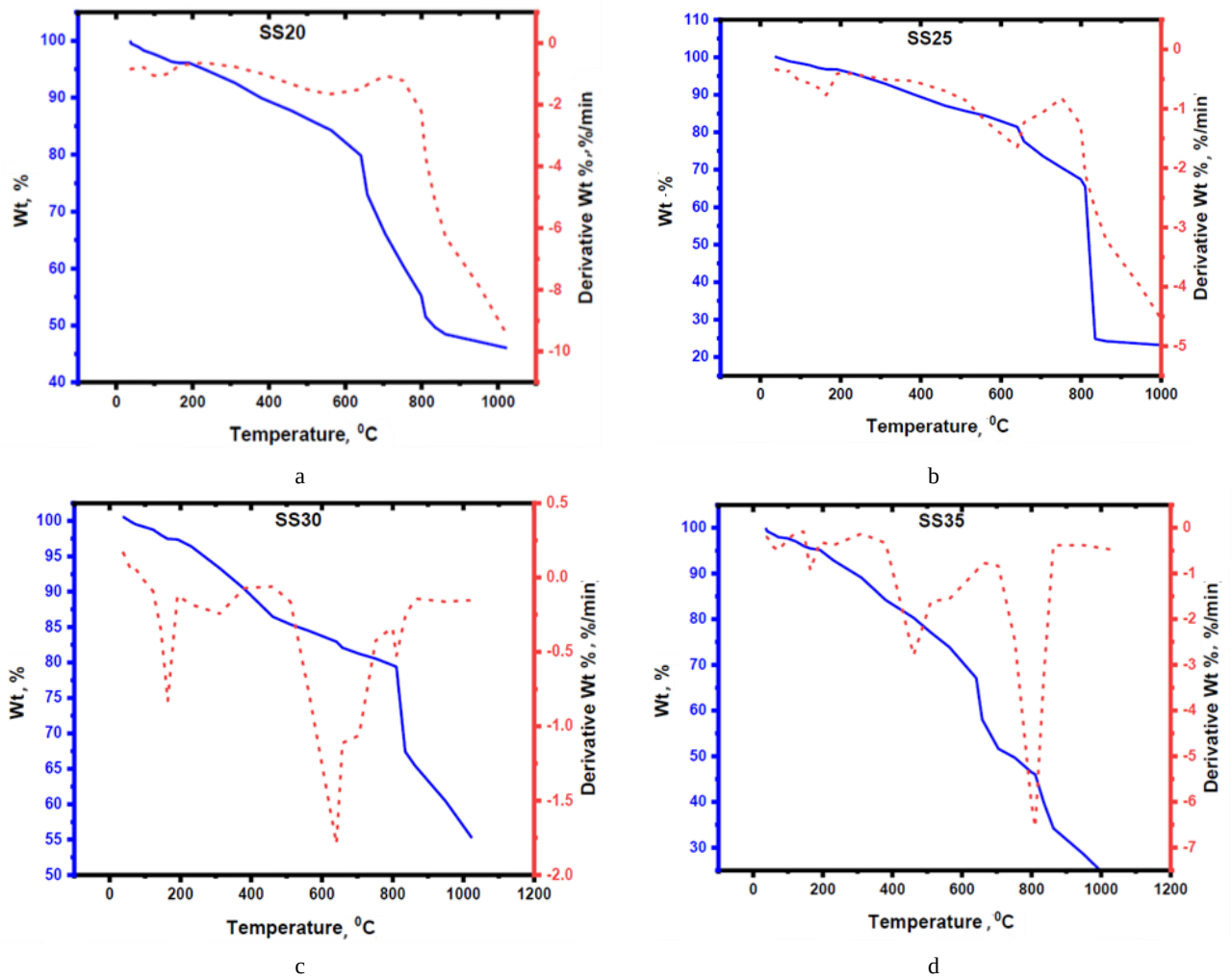

Fig. 8. TGA curves of brake pads: a – SS20; b – SS25; c – SS30; d – SS35

The reported range of temperatures at which deterioration occurs may be the result of differences in the materials that were used. Another degradation event was seen at around 900 °C, and it was determined that this one was caused by the transformation of $CaCO_3$ in the seashell into CaO. At a temperature of 810 °C, the $CaCO_3$ in seashells rapidly decomposes into CaO, which results in a considerable loss of mass for the shells. The objective of the research team that was responsible for this study was to develop a brake pad that was easier on the environment without compromising the pad's performance in terms of its thermal stability. It is important to note that seashells may be used to fill brake pads, and they can be used in a vehicle's braking system if the temperature does not exceed 460 °C.

3.4. Composition optimization

A loss function was used by Genichi Taguchi [39] and it is the difference between the experimental value and the goal value that is then turned back into the signal-to-noise ratio. The S/N ratio, often known as the mean to standard deviation ratio, is defined as follows: Taguchi referred to the desirable value (mean) for the response as the signal, and the unwanted value (standard deviation) for the response as the noise [40]. These terms reflect the response in their respective ways. Taguchi has split the S/N ratio into three categories, based on the needs of response. These categories include medium-the-better, higher-the-better, and lower-the-better. The range for each controllable parameter was chosen based on the results of the preliminary trials, which are detailed in Table 5.

Table 5. Composition process parameters and their levels

Composition parameters	Levels			
	1	2	3	4
Particle size, μm – A	100	115	125	140
Phenolic resin, wt.% – B	63	58	53	48
Sea shell powder, wt.% – C	20	25	30	35
Time, min – D	5	10	15	20

According to the findings of this research, a lower value for quality parameters such as wear rate ($R1$) and water absorption ($R2$) is preferable when trying to improve machinability.

$$\frac{S}{N} ratio\ (Smaller\ is\ better) = -10log\frac{1}{n}\sum(R)^2, \quad (1)$$

where n is the number of observations; R is the each observed data response.

Therefore, the above-mentioned Eq. 1 was used in order to compute the S/N ratio [41], and the results of this calculation are shown in Table 6. The Taguchi analysis was performed with the help of the Minitab 19.0 software tool

[42]. The findings of the analysis of variance (ANOVA), as well as the means of mean plot and the means of S/N ratio plots, were obtained and will be provided in the subsequent discussions.

Brake pad surfaces undergo deformation during contact, and certain abrasions might lead to excessive wear owing to the pads heterogeneous composition. The adhesion process destroys the pore walls and creates 1 – 2 μm high plateaus in the non-adherent zones. Fig. 9 depicts the major impact plot for the minimal wear rate. The longer line represents the most influential element, and the addition of the filler powder is shown next to it on the plot, which was constructed using the "smaller is better" aim [36].

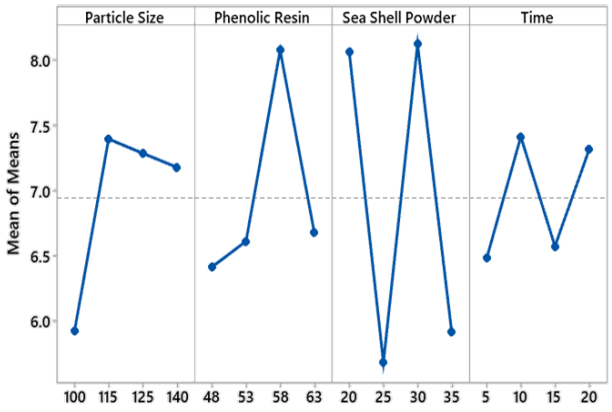

Fig. 9. Composition process parameters effects on wear rate *R*1

From the graph, it was observed that the SS powders added should be as high as possible; this variable has the most impact. Phenolic resin, which decomposes at about 450 °C, is the ideal binder for brake pad production. Utilizing a 100 μm sieve of SS powder with 70 % and 30 % composition of resin, the findings indicated superior results for the fabrication of brake pads than those seen in the literature for an asbestos brake pad using agrowaste and phenolic resin as binder [43]. The generated samples lost hardness, density, and compressive strength as the sieve grade became smaller, but the wear rate got larger. The brake pad materials improved characteristics may be attributed to its increasingly tiny sieve particle size. The present research evaluates the rate of wear on brake pads as well as their composition in the context of the above factors. In real world applications a braking system must function in wet, dusty, and oily environments. The brake pads must maintain consistent performance and minimal wear under these extreme circumstances. Friction composites must be inert in both water and oil. Consequently, it is necessary to measure the quantity of oil and water absorbed by the pads when they are immersed in both water and oil over a period. From Fig. 10 it is observed that more water and oil were absorbed by the brake pads that had SS shell additive material applied to them.

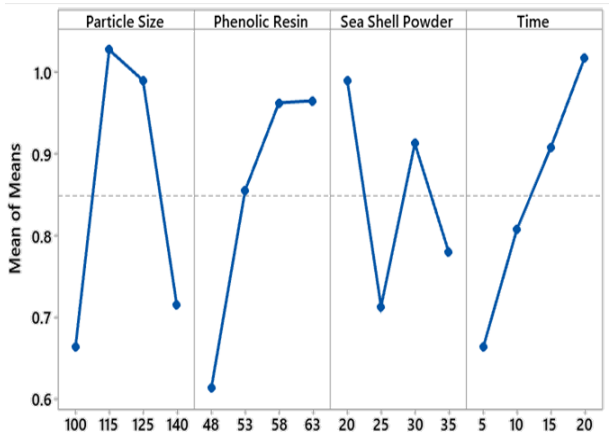

Fig. 10. Composition parameters effects on water absorption *R*2

The particle size of sea shell is claimed to change the properties of the formed brake pads, with a rise in hardness, compressive strength, and density as the particle size is reduced from 710 to 125 μm and a reduction in oil absorption, wear rate, and water absorption rate [28]. Therefore, the 125 μm sieve size of periwinkle shell particles produced results that were comparable to those produced by a commercial brake pad. A higher level of mechanical characteristics may be achieved by ensuring that the reinforcement is securely bonded to the matrix [44].

Table 6. Optimization plan, experimental results and S/N ratios

Run	Composition parameters				Experimental results		S/N ratios	
	A	B	C	D	Wear rate *R*1	Water absorption *R*2	*R*1	*R*2
1	1	1	1	1	6.29	0.73	−15.9730	2.7335
2	1	2	2	2	6.31	0.6	−16.0006	4.4370
3	1	3	3	3	6.37	0.79	−16.0828	2.0475
4	1	4	4	4	4.69	0.53	−13.4235	5.5145
5	2	1	2	3	5.46	1.07	−14.7439	−0.5877
6	2	2	1	4	10	1.45	−20.0000	−3.2274
7	2	3	4	1	5.62	0.78	−14.9947	2.1581
8	2	4	3	2	8.5	0.81	−18.5884	1.8303
9	3	1	3	4	8.63	1.34	−18.7202	−2.5421
10	3	2	4	3	7	1.09	−16.9020	−0.7485
11	3	3	1	2	8.51	1.1	−18.5986	−0.8279
12	3	4	2	1	5	0.43	−13.9794	7.3306
13	4	1	4	2	6.33	0.72	−16.0281	2.8534
14	4	2	3	1	9	0.71	−19.0849	2.9748
15	4	3	2	4	5.93	0.75	−15.4611	2.4988
16	4	4	1	3	7.45	0.68	−17.4431	3.3498

The findings of the current investigation are in accord with the literature provided, as shown in Fig. 10, which displays the influence of process parameters on water absorption.

Table 6 makes it simple to interpret the results of the experiment by bolding the values of the levels corresponding to the experimental conditions. An A1-B1-C2-D1 configuration is shown to be the most wear-resistant combination. Table 7 indicates the S/N response achieved for the *R*1. Fig. 11 shows the average signal-to-noise ratio calculated using the Minitab programme. A smaller S/N ratio indicates a larger discrepancy between the desired and actual output. From Fig. 11, it was found that the best mean S/N ratio for R1 was achieved with a particle size of 100 µm, a Phenolic resin concentration of 63 wt.%, a sea shell powder concentration of 30 wt.%, and a treatment period of 5 minutes. Therefore, A = 100 µm; B = 63 wt.%; C = 30 wt.% and D = 5 mins were determined to be the optimal process parameters for achieving a low wear rate, as anticipated by the Taguchi technique.

Table 7. Wear rate – mean S/N ratios

Composition parameters	Mean S/N ratios					
	Level 1	Level 2	Level 3	Level 4	Max-Min	Rank
Particle size, µm – A	–15.37	–17.08	–17.05	–17	1.71	3
Phenolic resin, wt.% – B	–15.86	–16.28	–18	–16.37	2.14	2
Sea shell powder, wt.% – C	–18	–15.05	–18.12	–15.34	3.07	1
Time, min – D	–16.01	–17.3	–16.29	–16.9	1.29	4

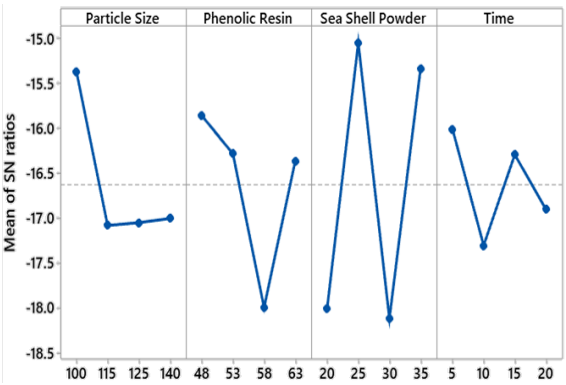

Fig. 11. Wear rate – mean S/N ratio

The S/N ratio response table for water absorption is shown in Table 8. The average S/N ratio for water absorption is graphically shown in Fig. 12 and A = 115 µm; B = 48 wt.%; C = 20 wt.% and D = 20 min were determined to be the projected optimal process parameters for achieving minimal water absorption. Water absorption was shown to be maximized with the predicted combination of elements A2-B4-C1-D4.

It is necessary to conduct conformance tests to verify Taguchi's predicted optimal conditions. Estimating and verifying the response at the predicted optimal composition and process parameters was accomplished with the help of the predicted S/N ratio (ε), which was computed with the help of Eq. 2 [45].

$$\varepsilon_{predicted} = \varepsilon_1 + \sum_{i=1}^{x}(\varepsilon_0 - \varepsilon_1), \quad (2)$$

where ε_1 is the mean S/N ratio (total); ε_0 is the optimum mean S/N ratio; x is the number of input process parameters.

Table 8. Water absorption – mean S/N ratios

Composition parameters	Mean S/N ratios					
	Level 1	Level 2	Level 3	Level 4	Max-Min	Rank
Particle size, µm – A	3.68	0.04	0.80	2.92	3.64	2
Phenolic resin, wt.% – B	4.51	1.47	0.86	0.61	3.89	1
Sea shell powder, wt.% – C	0.51	3.42	1.08	2.44	2.91	4
Time, min – D	3.80	2.07	1.02	0.56	3.24	3

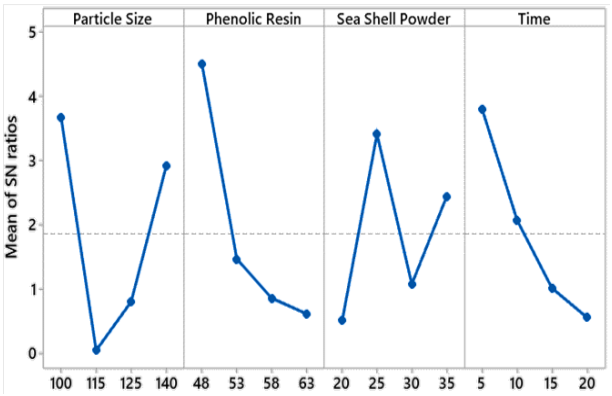

Fig. 12. Water absorption – mean S/N ratio

The confirmation tests were carried out using the composition and process parameters that Taguchi had predicted to be optimal. The results of these experiments are reported in Table 9 and Table 10 for *R*1 and *R*2 respectively. An increase in the performance characteristic findings may be attained by using the predicted optimal composition and process parameters for both *R*1 and *R*2.

Table 9. Wear rate conformation test

Parameters	Initial process parameters	Optimal parameters	
		Experimental	Predicted
Level	A_2-B_2-C_2-D_2	A_1-B_1-C_2-D_1	A_1-B_1-C_2-D_1
Wear rate	6.43	4.95	
S/N ratio	–15.7170	–13.0050	–12.9125
Improvement in S/N ratio	2.712		
Percentage reduction	52.4 %		

Table 10. Water absorption conformation test

Parameters	Initial process parameters	Optimal parameters	
		Experimental	Predicted
Level	A_2-B_2-C_2-D_2	A_2-B_4-C_1-D_4	A_2-B_4-C_1-D_4
Wear rate	0.87	0.59	
S/N ratio	4.743	2.616	2.4818
Improvement in S/N ratio	2.127		
Percentage reduction	31.4 %		

It was shown, using Table 9 and Table 10, that the S/N ratios of predicted optimum composition and process

parameters are rather similar for both $R1$ and $R2$. When compared to the original parameter values, the S/N ratio improvement achieved at the optimal composition and process parameters for $R1$ and $R2$ are 2.712 and 2.127 respectively. These data can be seen in Tables 9 and Table 10. It was discovered via the conformation tests that the Taguchi predicted optimal composition and process parameters delivers preferable outcomes in comparison to the initial parameter conditions in which $R1$ and $R2$ decrease were found to be 52.4 % and 31.4 % respectively when compared to starting parameter conditions. As a result, the Taguchi predicted optimal composition and process parameters were accepted as the optimum composition and process parameters for getting the low $R1$ and low $R2$ in machining of SS brake pads under the specified conditions. This was done to acquire the low $R1$ and low $R2$ values. Based on the findings, it was discovered that the Taguchi optimization approach considerably enhanced the machinability features of the SS brake pads while maintaining the same set of process settings.

Viewing discrete contours of the expected response variables allows for the creation of contour plots, which are used for analyzing the relationship between a response variable and two control variables. The contour plots that describe the association between the process parameters and wear rate value are shown in Fig. 13.

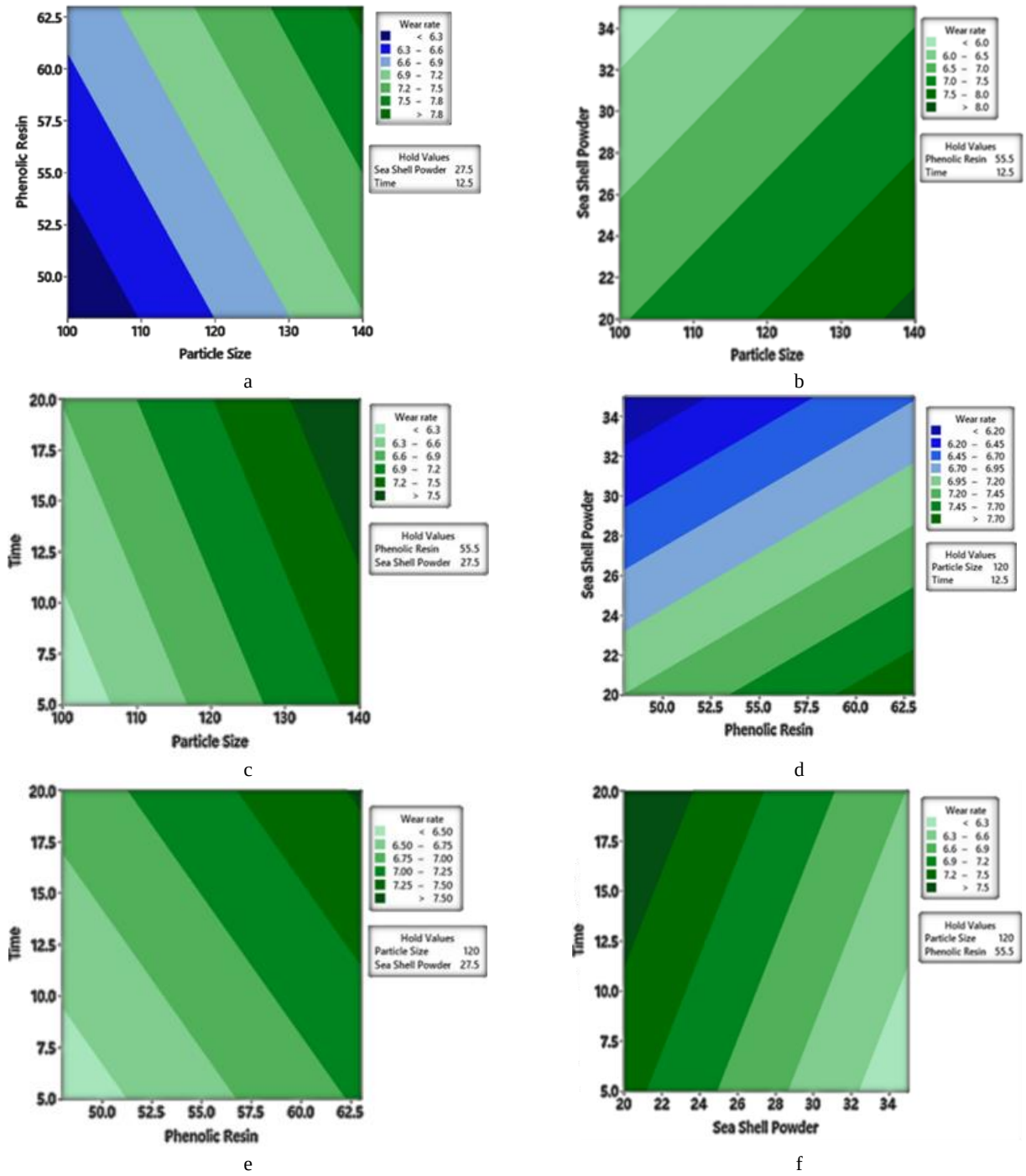

Fig. 13. Wear rate contour plots for: a – phenolic resin; b – sea shell powder vs particle size; c – for time vs particle size; d – for sea shell powder vs phenolic resin; e – time vs phenolic resin; f – time vs sea shell powder

According to what was discovered while examining Fig. 13 a, a combination of a high level of phenolic resin and a low level of particle size results in a low production of wear rate value. As shown in Fig. 13 b, a low wear rate could be achieved by having a high concentration of sea shell powder and large particle size levels accordingly. It was discovered, as shown in Fig. 13 f, that a little amount of time combined with a large amount of sea shell powder results in a low amount of wear. In a similar manner, the value of the wear rate decreased substantially over the course of time when high phenolic resin and low particle size were used, as shown in Fig. 13 c and e. However, as shown in Fig. 13 d, a high phenolic resin concentration and a high sea shell powder content both contribute to an increased rate of wear.

Fig. 14 displays contour plots that describe the correlation between the process parameters and the amount of water absorbed by the material. It was observed, using Fig. 14 b, d, and f, that a low level of water absorption was achieved at a low level of particle size and a low level of sea shell powder concentration accordingly. On the other hand, producing brake pad material with a low degree of water absorption requires a significant amount of time and phenolic resin. When all the machining conditions were compared, it was discovered that SS brake pads had minimal water absorption as shown in Fig. 14 a, c, and e. The scientific underpinnings for the finding have been broken out in earlier sections. In the body of research that was conducted, findings of a comparable kind were found in other materials that were not based on asbestos [46].

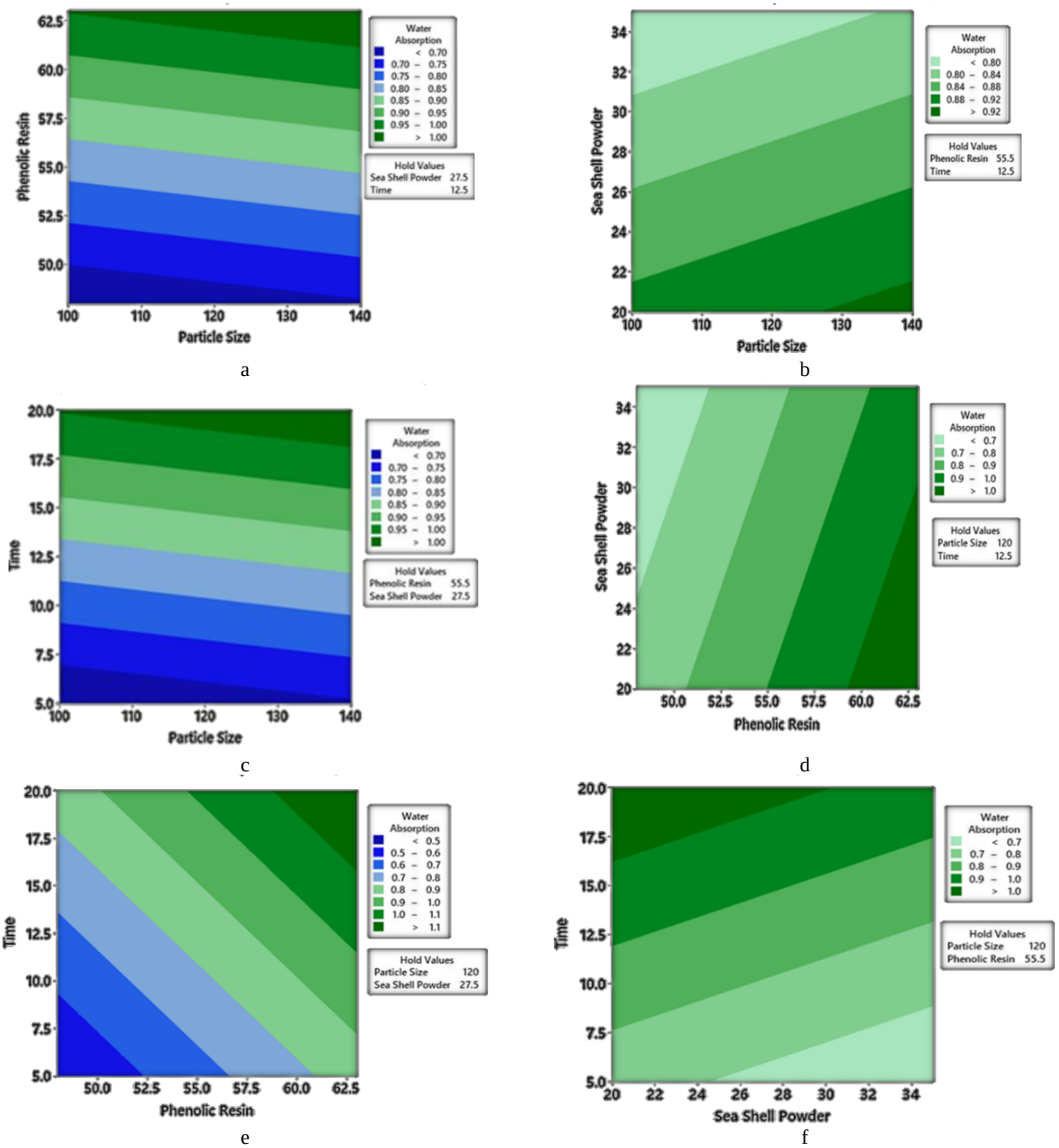

Fig. 14. Water absorption contour plots for: a – phenolic resin vs particle size; b – sea shell powder vs particle size; c – time vs particle size; d – sea shell powder vs phenolic resin; e – time vs phenolic resin; f – time vs sea shell powder

4. CONCLUSIONS

The complex brake friction materials used in the automobile industry was successfully developed using various ingredients for providing adequate performance properties.

1. Initially, four formulations were developed and fabricated with five ingredients by varying the compositions of sea shell (SS) powders as alternate for asbestos based brake pads, phenolic resin as binder and keeping other ingredients such as graphite as lubricant (5 wt.%), alumina as abrasive (7 wt.%) and stainless-steel powders (5 wt.%) as reinforcement were constant.
2. The first formulation contained 20 wt.% of sea shell (SS) powders and 63 wt.% of phenolic binder, the second formulation with 25 wt.% of sea shell (SS) powders and 58 wt.% of phenolic binder, the third formulation with 30 wt.% of sea shell (SS) powders and 53 wt.% of phenolic binder and the fourth formulation with 35 wt.% of sea shell (SS) powders and 48 wt.% of phenolic binder. All the developed brake pad materials are characterized for its physical, mechanical and tribological properties.
3. Morphological studies on worn surfaces showed that the major wear mechanisms throughout the braking process was abrasion, adhesion, grooving and delamination. It also showed that the friction layer was discontinuous and did not cover the whole surface. The sizes of the grooves depended on the sizes of the pull-out particles. From SEM micrographs, it was observed that the worn-out surfaces of the composite SS35 had the smooth surface with lesser cracks. Hence, the composite with 35 wt.% of SS powders (SS35) showed the best improvement in wear resistance.
4. It was observed that a high phenolic resin concentration and a high sea shell powder content both contribute to an increased rate of wear.
5. Multi-response optimization analysis on the fabrication of non-asbestos phenolic sea shell brake pads by composition of phenolic resin, sea shell powder, particle size and time were performed. Based on the experiments designed using Taguchi L16 array a set of non-linear regression equations were generated for wear rate and water absorption.
6. When all of the machining conditions were compared, it was discovered that SS brake pads had minimal water absorption.

These findings indicate that sea shell shows potential as an effective reinforcements in automotive brake pads delivering enhanced performance as compared to traditional brake pads.

Acknowledgements

This work was supported by the SEED grant received from Karpagam College of Engineering, Coimbatore, Tamilnadu, India granted on 29.09.2023. I'm grateful to Dr. Suresh Paramasivam for his insightful comments and feedback and to the staff at Karpagam College of Engineering, Coimbatore, for their technical assistance.

REFERENCES

1. **Achebe, C.H., Chukwuneke, J.L., Anene, F.A., Ewulonu, C.M.** A Retrofit for Asbestos Based Brake Pad Employing Palm Kernel Fiber as the Base Filler Material *Proceedings of the Institution of Mechanical Engineers, Part L: Journal of Materials: Design and Applications* 233 2019: pp. 1906 – 1913. https://doi.org/10.1177/1464420718796050
2. **Abutu, J., Lawal, S.A., Lafia Araga, R.A., Oluleye, M.A.** Microstructure and Thermal Analysis of Brake Pads Developed from Asbestos Free Materials *Arid Zone Journal of Engineering, Technology and Environment* 2020: pp. 375 – 386.
3. **Davide, C., Leonardi, M., Giovanni, S., Stefano, G.** Design of a Friction Material for Brake Pads Based on Rice Husk and its Derivatives *Wear* 2023: pp 526 – 527. http://dx.doi.org/10.1016/J.WEAR.2023.204893
4. **Chavhan, G.R., Wankhade, L.N.** Optimization of Test Parameters that Influence on Dry Sliding Wear Performance of Steel Embedded Glass/Epoxy Hybrid Composites by Using the Taguchi Approach *Tribology in Industry* 42 2020: pp. 556 – 571. https://doi.org/10.24874/ti.863.03.20.09
5. **Chinedu, O.K.** Optimization of Design Parameter for Coal Ash and Palm Kernel Shell Brake Pad Using Taguchi Experiment Design Method *International Journal of Innovation and Sustainability* 2 2018: pp. 66 – 72.
6. **Cho, M.H., Kim, S.J., Kim, D., Jang, H.** Effects of Ingredients on Tribological Characteristics of a Brake Lining: An Experimental Case Study *Wear* 258 2005: pp. 1682 – 1687. https://doi.org/10.1016/j.wear.2004:11.021
7. **Choi, Y.A., Lee, T.J., Kim, D.S.** Development of Source Profiles for Asbestos and Non-asbestos Fibers by SEM/EDX *Journal of Korean Society for Atmospheric Environment* 23 2007: pp. 718 – 726. https://doi.org/G704-000431.2007.23.6.006
8. **Jayashree, B., Mukesh, K.** Optimization of Steel Wool Contents in Non-asbestos Organic (NaO) Friction Composites for Best Combination of Thermal Conductivity and Tribo Performance *Wear* 263 (7 – 12) 2007: pp. 1243 – 1248. https://doi.org/10.1016/j.wear.2007.01.125
9. **Cho, M.H., Kim, S.J., Kim, D., Jang, H.** Effects of Ingredients on Tribological Characteristics of a Brake Lining: An Experimental Case Study *Wear* 258 (11 – 12) 2005: pp. 1682 – 1687. https://doi.org/10.1016/j.wear.2004.11.021
10. **Lenin Singaravelu, D., Vijay, R., Rahul, M.** Influence of Crab Shell on Tribological Characterization of Eco-Friendly Products Based Non-Asbestos Brake Friction Materials *SAE International* 2015: pp. 1 – 9. https://doi.org/10.4271/2015-01-2676.
11. **Almaslow, A., Ghazali, M.J., Talib, R.J., Ratnam, C.T., Azhari, C.H.** Effects of Epoxidized Natural Rubber Alumina Nanoparticles (ENRAN) Composites in Semi Metallic Brake Friction Materials *Wear* 302 2013: pp. 1392 – 1396. https://doi.org/10.1016/j.wear.2013.01.033
12. **Amirjan, M.** Microstructure, Wear and Friction Behavior of Nanocomposite Materials with Natural Ingredients *Tribology International* 131 2019: pp. 184 – 190. https://doi.org/10.1016/j.triboint.2018.10.040
13. **Anbunathan, P.E., Perumal, G., Senthilkumar, N.** Characterization and Wear Studies on Non-asbestos Organic

Fiber Reinforced Low Metallic Friction Composites *International Journal of Mechanical and Production Engineering Research and Development* 9 2019: pp. 133 – 143.

14. **Antonyraj, J., Vijay, R.** Influence of WS_2/SnS_2 on the Tribological Performance of Copper Free Brake Pads *Industrial Lubrication and Tribology* 71 2018: pp. 398 – 405. https://doi.org/10.1108/ILT-06-2018-0249
15. **Aranganathan, N., Mahale, V., Bijwe, J.** Effects of Aramid Fiber Concentration on the Friction and Wear Characteristics of Non-asbestos Organic Friction Composites Using Standardized Braking Tests *Wear* 354 2016: pp. 69 – 77. https://doi.org/10.1016/j.wear.2016.03.002
16. **Adeyemi, I.O., Nuhu, A.A., Thankgod, E.B.** Development of Asbestos Free Automotive Brake Pad Using Ternary Agro-waste Fillers *Journal of Multidisciplinary Engineering Science and Technology* 3 2016: pp. 5307 – 5323.
17. **Ahmed, K.A., Mohideen, S.H.R., Balaji, M.A.S., Sethupathy, P.B.** Synergic Effect of Metallic Fillers as Heat Dissipaters in the Tribological Performance of a Non-Asbestos Disk Brake Pad *Proceedings of the Institution of Mechanical Engineers, Part J: Journal of Engineering Tribology* 236 2022: pp. 292 – 301. https://doi.org/10.1177/13506501211018953
18. **Algan, I., Kurt, A.** The Effect of Metal Fibres and Borax Powders on the Wear and Friction Performances of the Organic Based Brake Pads *Metallofizika i Noveishie Tekhnologii* 39 2017: pp. 1511 – 1523. https://doi.org/10.15407/mfint.39.11.1511
19. **Ammar, Z., Ibrahim, H., Adly, M., Sarris, I., Mehanny, S.** Influence of Natural Fiber Content on the Frictional Material of Brake Pads – A Review *Journal of Composites Science* 7 (2) 2023: pp. 72. https://doi.org/10.3390/jcs7020072
20. **Jeyapragash, R., Srinivasan, V., Sathiyamurthy, S.** Mechanical Properties of Natural Fiber/Particulate Reinforced Epoxy Composites – A Review of the Literature, *Materials Today: Proceedings* 22 (3) 2020: pp. 1223 – 1227. https://doi.org/10.1016/j.matpr.2019.12.146
21. **Jaafar, T.R., Selamat, M.S., Kasiran, R.** Selection of Best Formulation for Semi-Metallic Brake Friction Materials Development *Powder Metallurgy* 2012: pp. 1 – 30. https://doi.org/10.13140/2.1.1222.2404
22. **Özsoy, M.İ., Türk, S., Fındık, F., Özacar, M.** Carbon–Carbon Nanocomposites for Brake Systems and Exhaust Nozzles *Nanotechnology in the Automotive Industry* 2022: pp. 131 – 154. https://doi.org/10.1016/B978-0-323-90524-4.00007-4
23. **Venugopal, S., Karikalan, L.** A Review Paper on Aluminium-Alumina Arrangement of Composite Materials in Automotive Brakes *Materials Today: Proceedings* 21 2020: pp. 320 – 323 https://doi.org/10.1016/j.matpr.2019.05.452
24. **Sankar, V.V.A., Suresh, P.** Asbestos-Free Brake Lining Material Using Sea Shell *Materiale Plastice.* 59 (3) 2022: pp. 100 – 108. https://doi.org/10.37358/MP.22.3.5609
25. **Blau, P.** Compositions, Functions, and Testing of Friction Brake Materials and Their Additives *Osti.Gov* 2001: pp. 1 – 23. https://doi.org/10.2172/788356
26. **Vijay, R., Sathyamoorthy, G., Vinod, A., Lenin Singaravelu, D., Sanjay, M.R., Siengchin, S.** Effective Utilization of Surface-Processed/Untreated Cardiospermum Halicababum Agro-Waste Fiber for Automobile Brake Pads and its Tribological Performance *Tribology International* 197 2024: pp. 109776. https://doi.org/10.1016/j.triboint.2024.109776
27. **Faga, MG., Casamassa, E., Iodice, V., Sin, A., Gautier, G.** Morphological and Structural Features Affecting the Friction Properties of Carbon Materials for Brake Pads *Tribology International* 140 2019: pp. 1 – 13. https://doi.org/10.1016/j.triboint.2019.105889
28. **Stephen, J.T., Oladokun, T., Adeyemi, G.J., Abere, J.** Effect of Particle Size on Mechanical Properties and Wear Behaviour of Brake Lining Produced from Waste Material: Sawdust *Journal of Current Engineering and Technology* 1 2019: pp. 1 – 8. https://doi.org/10.36266/JCET/108
29. **Singh, T., Patnaik, A., Chauhan, R., Bíró, I., Jánosi, E., Fekete, G.** Performance Assessment of Phenolic Based Non-Asbestos Organic Brake Friction Composite Materials with Different Abrasives *Acta Polytechnica Hungarica* 17 2020: pp. 49 – 67. https://doi.org/10.12700/APH.17.5.2020.5.3
30. **Wakasa, K., Matsui, H., Yamaki, M.** An Application of Non-asbestos Papers to the Dental Field: Mechanical Properties and Structural Change *Journal of Materials Science: Materials in Medicine*, 1990: pp. 177 – 181. https://doi.org/10.1007/BF00700879
31. **Ammar, Z., Ibrahim, H., Adly, M., Sarris, I., Mehanny, S.** Influence of Natural Fiber Content on the Frictional Material of Brake Pads – A Review *Journal of Composites Science* 7 (2) 2023: pp. 72. https://doi.org/10.3390/jcs7020072
32. **Dirisu, J.O., Okokpujie, I.P., Joseph, O.O., Oluwasegun Falodun., Lagouge K. Tartibu., Firdaussi D. Shehu.** Sustainable Biocomposites Materials for Automotive Brake Pad Application: An Overview *Journal of Renewable Materials* 12 (3) 2024: pp. 485-511. http://dx.doi.org/doi.org/10.32604/jrm.2024.045188
33. **Cai, R., Zhang, J., Nie, X., Tjong, J., Matthews, D.T.A.** Wear Mechanism Evolution on Brake Discs for Reduced Wear and Particulate Emissions *Wear* 452 2020: pp. 203 – 213. https://doi.org/10.1016/j.wear.2020.203283
34. **Manoharan, S., Krishnan, G.S., Babu, L.G., Vijay, R., Singaravelu, D.L.** Synergistic Effect of Red Mud-iron Sulfide Particles on Fade-recovery Characteristics of Non-asbestos Organic Brake Friction Composites *Materials Research Express* 6 2019: pp. 105311. https://doi.org/10.1088/2053-1591/ab366f
35. **Zhenyu, W., Jie, W., Fenghong, C.A.O., Yunhai, M.A.,** Comparative Braking Performance Evaluation of a Commercial and Non-asbestos, Cu-free, Carbonized Friction Composites *Materials Science* 27 2021: pp. 197 – 204. https://doi.org/10.5755/j02.ms.2352
36. **Kahraman, F., Sugözü, B.** An integrated Approach Based on the Taguchi Method and Response Surface Methodology to Optimize Parameter Design of Asbestos-Free Brake Pad Material *Turkish Journal of Engineering* 3 2019: pp. 127 – 132. http://dx.doi.org/10.31127/tuje.479458
37. **Md, J.S., Madhu, S., Chakravarthy, K.S., Siva Naga Raju, J.** Characterization of Natural Cellulose Fibers from the Stem of Albizia Julibrissin as Reinforcement for Polymer

Composites *Journal of Natural Fibers* 19 (6) 2022: pp. 2204 – 2217. https://doi.org/10.1080/15440478.2020.1807440

38. **Frédéric, M., Luquet, G.** Molluscan Shell Proteins *Comptes Rendus Palevol* 3 (6 – 7) 2004: pp. 469 – 492. https://doi.org/10.1016/j.crpv.2004.07.009
39. **Yusubov, F.F.** Wear Studies on Phenolic Brake-Pads Using Taguchi Technique *Tribology in Industry* 43 2021: pp. 489 – 499. https://doi.org/10.24874/ti.1024.12.20.03
40. **Vaibhav, K., Hrishikesh, K.** Taguchi Method Optimization of Operating Parameters for Automotive Disc Brake Pad Wear *Applied Engineering Letters: Journal of Engineering and Applied Sciences* 6 2021: pp. 47 – 53. https://doi.org/10.18485/aeletters.2021.6.2.1
41. **Shagwira, H., Mbuya, TO., Mwema, F.M., Herzog, M., Akinlabi, ET.** Taguchi optimization of surface roughness and material removal rate in CNC milling of polypropylene+ 5wt.% quarry dust composites *IOP Conference Series: Materials Science and Engineering* 1107 2021: pp. 1 – 9. http://dx.doi.org/10.1088/1757-899X/1107/1/012040
42. **Chavhan, G.R., Wankhade, L.N.** Optimization of test Parameters that Influence on Dry Sliding Wear Performance of Steel Embedded Glass/Epoxy Hybrid Composites by Using the Taguchi Approach *Tribology in Industry* 42 2020: pp. 556 – 571. http://dx.doi.org/10.24874/ti.863.03.20.09
43. **Lawal, S.S., Ademoh, N.A., Bala, K.C., Abdulrahman, A.S.** Reviews in Automobile Brake Pads Production and Prospects of Agro Base Composites of Cashew Nut Shells and Nigerian Gum Arabic Binder *Covenant Journal of Engineering Technology* 3 2019: pp. 102 – 134. https://journals.covenantuniversity.edu.ng/index.php/cjet/article/view/1797
44. **Young, R.J., Kinloch, I.A., Gong, L., Novoselov, KS.** The Mechanics of Graphene Nanocomposites: A Review *Composites Science and Technology* 72 2012: pp. 1459 – 1476. https://doi.org/10.1016/j.compscitech.2012.05.005
45. **Sunil, D., Suresh Kumar Reddy, N.** Optimizing Turning Parameters in the Machining of AM Alloy Using Taguchi Methodology *Measurement* 169 2021: pp.1 – 8. https://doi.org/10.1016/j.measurement.2020.108340
46. **Saravanakumar, P., Dhanasekhar, S.** Study And Analysis of Silicon Carbide Particles Reinforced With Al 6061 Metal Matrix Composites of Brake Rotor using Pin-On-Disc *International Journal of Advanced Research in Engineering and Technology* 12 (1) 2021: pp. 1150 – 1166. https://doi.org/10.34218/IJARET.12.1.2021.10